Soft Matter

Effect of local active fluctuations on structure and dynamics of flexible biopolymers

Journal:	*Soft Matter*
Manuscript ID	SM-ART-11-2023-001491.R1
Article Type:	Paper
Date Submitted by the Author:	21-Dec-2023
Complete List of Authors:	Dutta, Sayantan; Stanford University, Chemical Engineering Ghosh, Ashesh; Stanford University, Chemical Engineering Spakowitz, Andrew; Stanford University, Chemical Engineering

Soft Matter

ARTICLE TYPE

Cite this: DOI: 00.0000/xxxxxxxxxx

Effect of local active fluctuations on structure and dynamics of flexible biopolymers†

Sayantan Dutta,[a] Ashesh Ghosh,[a] and Andrew J. Spakowitz[a,b,c,*]

Received Date
Accepted Date

DOI: 00.0000/xxxxxxxxxx

Active fluctuations play a significant role in the structure and dynamics of biopolymers (*e.g.* chromatin and cytoskeletal proteins) that are instrumental in the functioning of living cells. For a large range of experimentally accessible length and time scales, these polymers can be represented as flexible chains that are subjected to spatially and temporally varying fluctuating forces. In this work, we introduce a mathematical framework that correlates the spatial and temporal patterns of the fluctuations to different observables that describe the dynamics and conformations of the polymer. We demonstrate the power of this approach by analyzing the case of a point fluctuation on the polymer with an exponential decay of correlation in time with a finite time constant. Specifically, we identify the length and time scale over which the behavior of the polymer exhibits a significant departure from the behavior of a Rouse chain and the range of impact of the fluctuation along the chain. Furthermore, we show that the conformation of the polymer retains the memory of the active fluctuation from earlier times. Altogether, this work sets the basis for understanding and interpreting the role of spatio-temporal patterns of fluctuations in the dynamics, conformation, and functionality of biopolymers in living cells.

1 Introduction

Biological polymers in living cells are subjected to active forces that play a pivotal role in numerous essential life processes. Various proteins, such as chromatin remodeling complexes, topoisomerases, and RNA polymerase, exert forces that modify chromatin structure, thereby enhancing or obstructing the transcription of specific genes[1,2,3,4,5,6,7]. Transcription factors bind to specific sites within chromatin through specific binding and unbinding rates[8,9], leading to forces that vary along the chromatin fiber. Cytoskeletal elements, such as actin filaments, are acted upon by molecular motors to create the contractile apparatus of a cell—a crucial component for functions ranging from cell crawling to muscle stretching[10,11,12,13,14,15]. The development of a robust physical framework is necessary to understand the impact of these active fluctuations on biopolymer structure and dynamics and to gain a comprehensive mechanistic understanding of the biological functions they serve.

Parallel to our growing understanding of biopolymer dynamics and structure through state-of-the-art experimental techniques, there have been numerous efforts in recent decades to model the active fluctuations occurring on polymers. On one hand, filament-like polymers are categorized as semiflexible and forced by tangential propulsion by molecular motors or self-propulsion of the monomers, leading to hydrodynamic interactions with their ambient fluids and the emergence of large-scale coherent flows[16,17,18,19,20,21,22,23]. On the other hand, biopolymers like chromatin have lengths significantly surpassing their persistence lengths and are effectively modeled as flexible polymers. While understanding the multi-scale behavior of chromatin requires consideration of inter-bead interactions, and evaluating chromosomal structure at nucleosome resolution necessitates accounting for bending rigidity[24,25,26,27,28], flexible polymer models consistently capture meso-scale dynamics[29,30,31,32,33] and can accommodate environmental viscoelasticity[30,34,35], architectural looping[32,36], and hydrodynamics[37,38]. Active fluctuations acting on flexible polymers are typically regarded as stochastic perturbations from the surroundings, affecting all chain monomers non-specifically[37,38,39,40,41,42]. However, these models do not assess the impact of active fluctuations localized to specific sites on the biopolymer. Previous studies leveraging theoretical analyses[43] and simulations[44] capture the influence of localized active forces on polymer structure, revealing elongation and swelling of the polymer chain due to the localized fluctuations.

We present a general framework in this paper that extends the physical behavior of flexible polymers[45] to incorporate fluc-

*Departments of [a]Chemical Engineering, [b] Material Science and Engineering, and [c] Biophysics Program, Stanford University, Stanford, California, U.S.A, 94305. *ajspakow@stanford.edu.*

† Electronic Supplementary Information (ESI) available: [details of any supplementary information available should be included here]. See DOI: 10.1039/cXsm00000x/

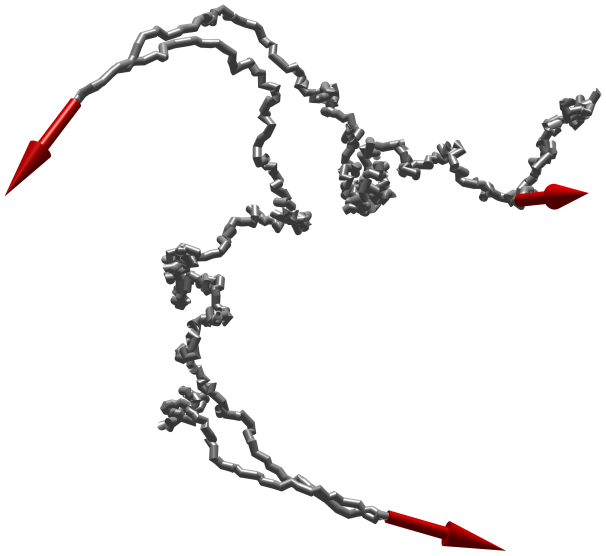

Fig. 1 Conformation of a flexible polymer chain subject to local active fluctuations. The gray curve represents the three dimensional conformation of the chain and the red arrows denote the unit vectors in the direction of the active fluctuation.

tuations that are correlated to bead positions. We allow these fluctuations to have a generic temporal correlation to account for their non-thermal nature. Our subsequent analyses focus on active fluctuations localized at specific sites along the polymer, characterized by a finite temporal persistence with a well-defined timescale. These results complement previous studies[43,44] by analyzing the multiscale dynamics of the polymer chain. We highlight how these active fluctuations influence polymer dynamics across various timescales and its structure at different length scales, depending upon their proximity to the source of the fluctuations. We also explore how the direction of these active fluctuations alters the polymer conformation. In this work, we specifically emphasize on how different experimental observables reveal the presence of a site on a polymer undergoing active fluctuations, its position along the polymer chain, and the characteristic timescale governing the persistence of these fluctuations.

2 Model and Theory

We outline the model to predict the dynamics of a flexible polymer chain in a viscous medium subject to Brownian and active fluctuations with a general spatio-temporal pattern (Fig. 1). We define a polymer chain as a space curve $\vec{r}(n,t)$ with monomer position n that runs from 0 at one end of the chain to the total chain length N, defined as the number of Kuhn lengths b in the polymer. In this model, the position of the nth segment of the polymer $\vec{r}(n,t)$ evolves according to the Langevin equation of motion[45]

$$\xi\frac{\partial\vec{r}(n,t)}{\partial t}=\frac{3k_BT}{b^2}\frac{\partial^2\vec{r}(n,t)}{\partial n^2}+\vec{f}^{\mathrm{B}}(n,t)+\vec{f}^{\mathrm{A}}(n,t), \tag{1}$$

where ξ is the coefficient of viscous drag on a monomer segment. This treatment of the viscous drag neglects long-range hydrodynamic interactions, which tend to be screened and negligible within the crowded environment in a living cell. However, changes within the environment that alter the degree of crowding may necessitate a more refined model for hydrodynamic interactions[37,38].

The Brownian force $\vec{f}^{\mathrm{B}}$ arises from thermal fluctuations at temperature T and is governed by the fluctuation dissipation theorem, written as

$$\langle\vec{f}^{\mathrm{B}}(n,t)\vec{f}^{\mathrm{B}}(n',t')\rangle=2k_BT\xi\,\delta(n-n')\delta(t-t')\mathbf{I}, \tag{2}$$

where $\mathbf{I}$ is the identity matrix[45]. We define the spatio-temporal correlation of the active fluctuations as

$$\langle\vec{f}^{\mathrm{A}}(n,t)\vec{f}^{\mathrm{A}}(n',t')\rangle=k_BT\xi Z(n,n')\kappa(|t-t'|)\mathbf{I}, \tag{3}$$

where $Z(n,n')$ and $\kappa(|t-t'|)$ respectively define the spatial and temporal correlation of the active fluctuation normalized by the thermal fluctuation. The boundary conditions reflecting the force-free condition at both the chain ends $\frac{\partial\vec{r}(n,t)}{\partial n}(n=0,t)=\frac{\partial\vec{r}(n,t)}{\partial n}(n=N,t)=0$.

The configuration of a flexible polymer is often studied as a linear superposition of orthonormal modes, which are eigenfunctions associated with Eq. 1 and are defined as

$$\phi_p(n)=\begin{cases}1 & p=0\\ \sqrt{2}\cos\left(\frac{pn\pi}{N}\right) & p>0.\end{cases} \tag{4}$$

The time-dependent amplitude of the pth mode can be calculated as $\vec{X}_p(t)=N^{-1}\int_0^N\vec{r}(n,t)\phi_p(n)\mathrm{d}n$. An inner product of Eq. 1 with the p^{th} eigenmode gives us the equation of motion of amplitude of the p^{th} eigenmode

$$N\xi\frac{\mathrm{d}\vec{X}_p}{\mathrm{d}t}=-\frac{3p^2\pi^2k_BT}{Nb^2}\vec{X}_p+\vec{f}_p^{\mathrm{B}}(t)+\vec{f}_p^{\mathrm{A}}(t), \tag{5}$$

where $\vec{f}_p^{\mathrm{B}}(t)=\int_0^N\vec{f}^{\mathrm{B}}(n,t)\phi_p(n)\mathrm{d}n$ and $\vec{f}_p^{\mathrm{A}}(t)=\int_0^N\vec{f}^{\mathrm{A}}(n,t)\phi_p(n)\mathrm{d}n$. From Eqs. 2 and 3 respectively, the correlation between the p^{th} and q^{th} eigencomponent of the fluctuation is given by $\langle\vec{f}_p^{\mathrm{B}}(t)\vec{f}_q^{\mathrm{B}}(t')\rangle=2k_BTN\xi\,\delta_{pq}\delta(t-t')$ and $\langle\vec{f}_p^{\mathrm{A}}(t)\vec{f}_q^{\mathrm{A}}(t')\rangle=k_BTN\xi L_{pq}\kappa(|t-t'|)$, where $L_{pq}=N^{-1}\int_0^N\int_0^N Z(n,n')\phi_p(n)\phi_q(n')\mathrm{d}n'\mathrm{d}n$.

We now determine the time-correlation of modal amplitudes, defined as $C_{pq}(t)=\langle\vec{X}_p(t)\cdot\vec{X}_q(0)\rangle$. Using Eq. 5 and properties of fluctuating forces, $\vec{f}_p^{\mathrm{B}}$ and $\vec{f}_p^{\mathrm{A}}(t)$, we derive (Supplementary Material note 1) that for $\{p,q\}>0$

$$C_{pq}(\tau)=\frac{Nb^2}{\pi^2}\exp(-p^2\tau)\left[\frac{\delta_{pq}}{p^2}+\right. \tag{6}$$

$$\left.L_{pq}\tau_R\int_{-\infty}^{\tau}\int_{-\infty}^{0}\mathrm{d}\tau_2\mathrm{d}\tau_1\exp\left(p^2\tau_1+q^2\tau_2\right)\kappa(|\tau_1-\tau_2|)\right],$$

where $\tau_R = \xi N^2 b^2/(3\pi^2 k_B T)$ is the characteristic time of relaxation of the longest wavelength mode of the chain (i.e. $p = 1$), often referred to as the Rouse time, and time is non-dimensionalized as $\tau = t/\tau_R$. We note that for a general function $Z(n,n')$, L_{pq} can be non-zero for $p \neq q$, suggesting coupled motion of different modes that is not exhibited in the absence of active forces.

In this article, we focus on active fluctuations at a specific segment n_0 with exponentially decaying temporal correlation, similar to an Ornstein–Uhlenbeck process[43,46,47,48] often used to describe active processes in biological context. Specifically, we define

$$Z(n,n') = N\Gamma\delta(n-n_0)\delta(n'-n_0) \quad (7)$$

$$\kappa(t,t') = t_A^{-1}\exp\left(-|t-t'|/t_A\right). \quad (8)$$

We define Γ to represent the ratio of the squared strength of total active and Brownian fluctuations on the polymer, and t_A is the timescale of persistence of the active fluctuation. This definition of spatio-temporal correlation in Eq. 6 leads to (see Supplementary Material note 1)

$$C_{pq}(\tau) = \frac{Nb^2}{\pi^2}\left\{\frac{\delta_{pq}}{p^2}\exp(-p^2\tau) + \frac{\Gamma k_A \phi_p(n_0)\phi_q(n_0)}{(k_A - p^2)}\left[\frac{2k_A}{(p^2+q^2)}\frac{\exp(-p^2\tau)}{(k_A+p^2)} - \frac{\exp(-k_A\tau)}{(k_A+q^2)}\right]\right\}, \quad (9)$$

where $k_A = \tau_R/t_A$. In the following section, we utilize this expression to study the impact of the point active fluctuation at the middle of the chain (i.e. $n_0 = 0.5N$) on the structure and dynamics of the polymer as a function of Γ and k_A, two dimensionless parameters representing the strength and timescale of the fluctuations, respectively.

3 Results

The theoretical foundation established in the preceding section allows us to calculate several statistical quantities related to conformation and dynamics of polymers. These quantities can be observed from the cutting-edge experimental tools utilized to study structure and dynamics of biopolymers such as chromatin.

3.1 Effect of local active fluctuation on dynamics

We begin our analysis with the mean squared displacement (MSD) of a tagged segment n of the polymer in time t. This quantity is captured from live imaging of a marker attached to a specific site along a chromosome[30,34,49]. The MSD has contributions from both the center of mass fluctuations (i.e. $p = 0$) as well as internal fluctuations in the structure (i.e. $p > 1$), such that

$$\begin{aligned} \mathrm{MSD}(n,t) &= \langle[\vec{r}(n,t) - \vec{r}(n,0)]^2\rangle \\ &= \left\langle\left[\vec{r}_{\mathrm{com}}(t) - \vec{r}_{\mathrm{com}}(0)\right]^2\right\rangle + \\ &\quad 2\sum_{p=1}^{\infty}\phi_p(n)\left\langle\left[\vec{r}_{\mathrm{com}}(t) - \vec{r}_{\mathrm{com}}(0)\right]\cdot\left[\vec{X}_p(t) - \vec{X}_p(0)\right]\right\rangle + \\ &\quad \sum_{p=1}^{\infty}\sum_{q=1}^{\infty}\phi_p(n)\phi_q(n)\left[2C_{pq}(0) - C_{pq}(t) - C_{qp}(t)\right]. \end{aligned} \quad (10)$$

For the specific case of active fluctuation at a point source with exponential decay of correlation with time (Eq. 8), we use the C_{pq}

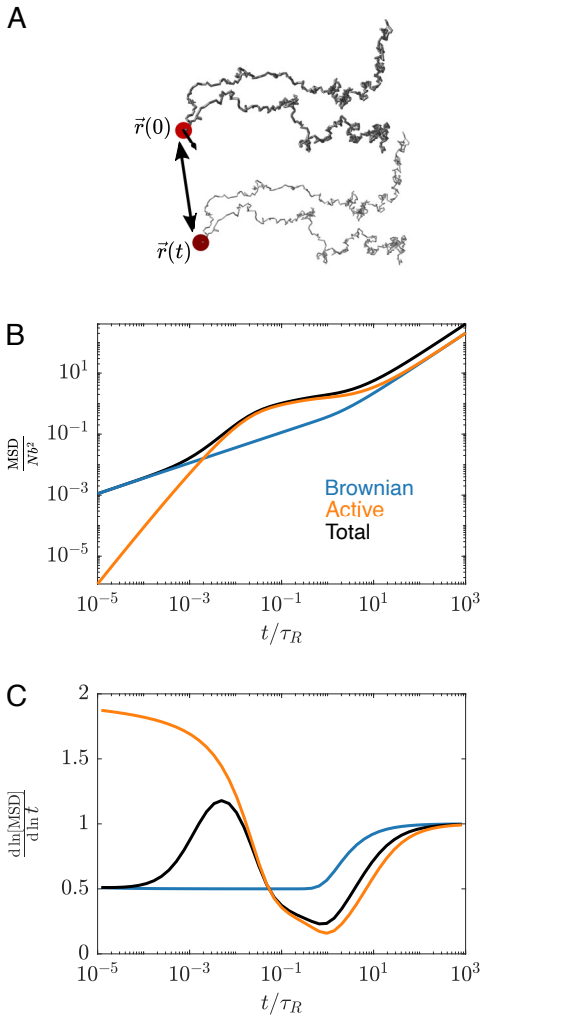

Fig. 2 (A) A schematic of a polymer at time 0 (thick line) and t (thin line), where the red point denotes the segment subject to active fluctuation, the arrow denotes the direction of active force, and the double arrow denotes the magnitude of the displacement of the segment in time t. (B) Mean squared displacement (MSD) and (C) apparent slope on a logarithmic scale as a function of time for a polymer subject to active fluctuation at the middle of the chain (i.e. $n_0 = 0.5N$) and characterized by $\Gamma = 1$,and $k_A = 100$. The black, blue, and orange curves denote the total MSD and the contributions of the Brownian and active fluctuations, respectively.

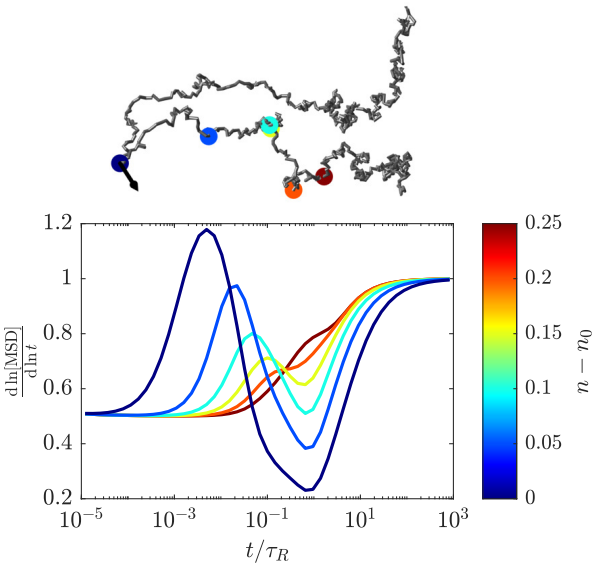

Fig. 3 The slope of MSD as a function of time for different segments. The color of the plot denotes the distance from the source of active fluctuation as shown in the colorbar. In the schematic above the plot, segments are labeled with their respective color in the plot. The source of the active fluctuation is denoted with an arrow.

from Eq. 9 for the contributions of internal fluctuations to derive the center of mass contributions to be (Supplementary Material note 2)

$$\left\langle [\vec{r}_{\rm com}(\tau) - \vec{r}_{\rm com}(0)]^2 \right\rangle = \frac{2Nb^2}{\pi^2}\left[(1+\Gamma)\,\tau + \frac{\Gamma}{k_A}\left[\exp(-k_A\tau) - 1\right]\right], \tag{11}$$

$$\left\langle [\vec{r}_{\rm com}(\tau) - \vec{r}_{\rm com}(0)] \cdot \left[\vec{X}_p(\tau) - \vec{X}_p(0)\right] \right\rangle = Nb^2\Gamma k_A \phi_p(n_0)\left[\frac{2k_A[1-\exp(-p^2\tau)] - 2p^2[1-\exp(-k_A\tau)]}{p^2\pi^2(k_A^2 - p^4)}\right], \tag{12}$$

where $\tau = t/\tau_R$.

First, we focus on the dynamics of the segment that itself is subject to active fluctuations (Fig. 2A). Our theory predict a significant enhancement in segmental dynamics in comparison to its Brownian-only counterpart, and the dynamics exhibit dramatic transitions across time scales (Fig. 2B). To illustrate the transitions further, we plot the local power-law scaling of the MSD in Fig. 2C. At very short times, the MSD follows a $t^{0.5}$ scaling. Then, the slope increases from 0.5, followed by a subsequent decay, and finally trending back to a scaaling t^1 at very long times (Fig. 2C).

We investigate this transition further by decomposing the MSD into Brownian (i.e. $\Gamma = 0$) and active components. Similar to a Rouse chain, the Brownian component shows a $t^{0.5}$ scaling at short times, and at $t > \tau_R$, it exhibits a scaling of t^1. On the other hand, the active component approaches a ballistic behavior (i.e. t^2 scaling) at very short times. The active scaling loses its ballistic nature at time scales where the active fluctuations decorrelate (i.e. at times $t > t_A = k_A^{-1}\tau_R$), eventually approaching a scaling of t^1 at $t > \tau_R$. The total MSD significantly deviates from the Brownian MSD under conditions where the active MSD dominates over Brownian MSD. We show that, at the short time, the Brownian MSD scales as $\sqrt{t/\tau_R}$. Whereas, the active MSD scales as $\Gamma k_A^2 (t/\tau_R)^2$, suggesting a time scale of transition $\sim (\Gamma k_A^2)^{-2/3}\tau_R$. The slope of the logarithm of total MSD decays again when the active MSD loses its ballistic nature in $k_A^{-1}\tau_R$. Finally in $t > \tau_R$, the active and Brownian MSD approach a scaling of t, and the polymer behaves like a Rouse chain with an enhanced effective temperature [i.e. $T(1+\Gamma)$].

Next, we investigate the effect of the active fluctuation in the dynamics of the segments which are not subject to active fluctuations. In Fig. 3, we show the power-law scaling of the MSD for segments at different distances from the source of the active fluctuation. We observe non-monotonic behavior in the MSD scaling similar to the predicted behavior at the active source in Fig. 2. However, the deviation from the Brownian behavior is delayed and less prominent as we move further away from the active source. The result suggests that from long-time live imaging of multiple tracers on a biopolymer at different locations, we can estimate the position of active sources by identifying the tracers that show fastest and most significant deviation from the Brownian MSD.

3.2 Effect of local active fluctuation on conformation

We study the effect of active fluctuations on the local conformation of the polymer. Specifically, we focus on the inter-spot distance between two specific segments on the polymer. This quantity can also be captured experimentally from live imaging of two or more fluorescent markers postioned at specific locations along the chromosome[49,50] or from multiple optical reconstruction of polymer structures from fixed imaging[51,52]. We show that the ensemble average of squared distance between two spots centered around the segment at $\bar{n}$ and separated by δ segment (Fig. 4A) is given by

$$\left\langle \Delta\vec{r}^2(\bar{n},\delta) \right\rangle = \sum_{p=1}^{\infty}\sum_{q=1}^{\infty} C_{pq}(0)\Delta\phi_p(\bar{n},\delta)\Delta\phi_q(\bar{n},\delta), \tag{13}$$

where $\Delta\phi_p(\bar{n},\delta) = \phi_p(\bar{n}+\delta/2) - \phi_p(\bar{n}-\delta/2)$. In Fig. 4B, we plot the mean squared distance between two points centered at a fixed point but with different segment length between them and show the contributions of the Brownian and active fluctuations separately. The mean squared distance between two segments for a flexible chain only subject to Brownian fluctuation (i.e. a Rouse chain) is proportional to the number of Kuhn segment between them (i.e. $\langle \Delta r^2 \rangle = \delta b^2$). On the other hand, the contribution from the active fluctuation scales with the square of the number of segments between them suggesting an elongated structure in a specific direction. Near the source of active fluctuation the active contribution scales as $\sim (\Gamma k_A/N)\delta^2 b^2$. These scaling relations suggest that the contribution of the active fluctuations to the conformation dominates over the Brownian contribution only beyond a critical length scale $\delta^* = N/\Gamma k_A$. We note that for the well-studied case of a flexible polymer chain subject to a force or a flow in a specific direction, the critical length-scale is also inversely propor-

tional to the square of the magnitude of the force[53,54,55].

Subsequently, we calculate the inter-spot distance of spots separated by same segment distance but centered at different positions (Fig. 4C). Our calculation shows that the inter-spot distance decreases as we move away from the source of the fluctuation. Whereas in the absence of any local active fluctuation, the distance is same irrespective of where the spots are centered. The length scale of the decay of the inter-spot distance gives us an estimate of the range of influence of the active fluctuation from its source. Specifically, we define this length scale to be $w_{1/2}$, where the mean squared inter-spot distance is the geometric mean of the mean squared inter-spot distances at the source of active fluctuations and the mean squared inter-spot distance for a Rouse chain given by

$$\left\langle \Delta\vec{r}^2(w_{1/2},\delta)\right\rangle = \frac{1}{2}\left[\left\langle \Delta\vec{r}^2(n_0+\delta/2,\delta)\right\rangle + \delta b^2\right]. \qquad (14)$$

We find that $w_{1/2}$ is insensitive to Γ, and is proportional to $k_A^{-1/3}$ for sufficiently small δ (Fig. 4C inset) suggesting that a local active fluctuation persisting for longer time (i.e. lower k_A) has a longer range of influence from the source. Altogether, these results show that local active fluctuations create elongated structures around the active source in comparison to the rest of the chain.

Next, we examine the effect of local active fluctuations on the global structure of the polymer. We quantify the swelling of the polymer due to the local active fluctuations by calculating the square of the radius of gyration in excess of the squared radius of

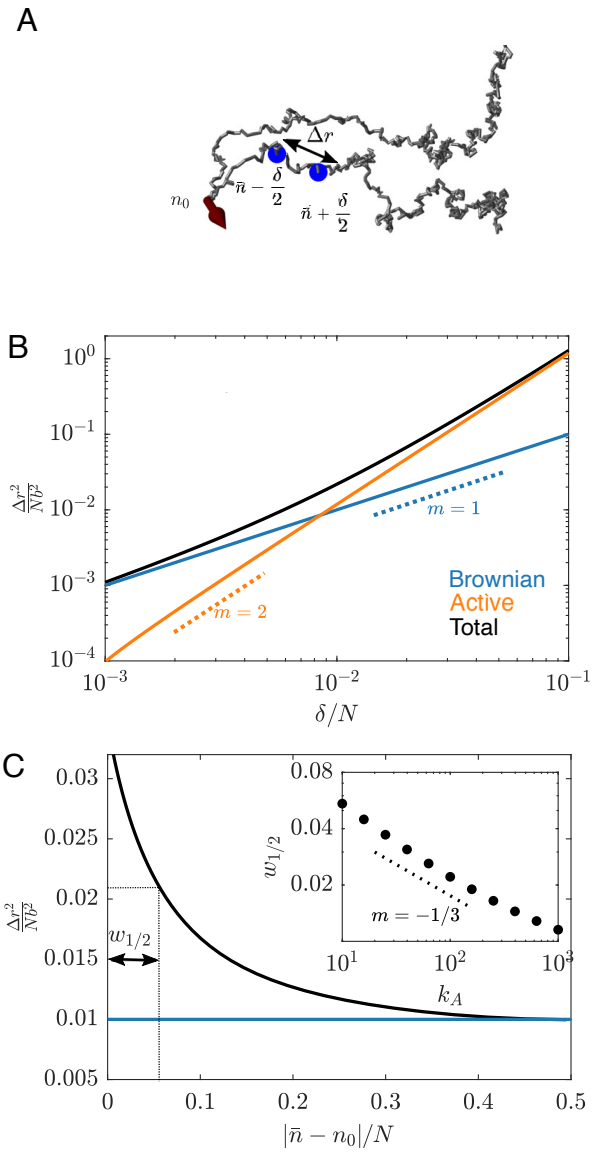

Fig. 4 (A) A schematic showing distance Δr between two tracers (blue) on a polymer chain separated by segment length δ centered at $\bar{n}$ subject to active fluctuations (red arrow) at the segment n_0. (B) Mean squared inter-spot distance Δr^2 as a function of segment distance (δ) between the spots for $\bar{n}=0.45N$, $n_0=0.5N$, $\Gamma=10$, and $k_A=10$. The three curves show the total mean squared inter-spot distance (black) and the contributions from Brownian (blue) and active (orange) fluctuations. The Brownian and active fluctuations exhibit scalings of δ and δ^2 respectively. (C) The black curve shows mean squared inter-spot distance Δr^2 separated by $\delta = 0.01N$ as a function of $\bar{n}$ for $\Gamma=10$ and $k_A=10$. The double arrow denotes the segment distance $w_{1/2}$, denoting the distance at half maximum. The inset shows a plot of $w_{1/2}$ as a function of k_A, exhibiting a scaling of -1/3 power.

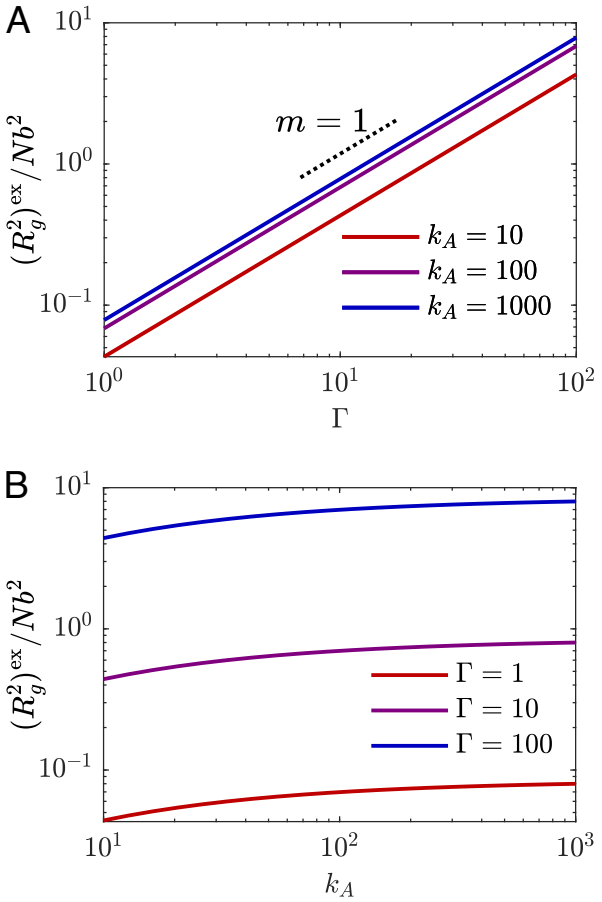

Fig. 5 Excess squared Radius of gyration (A) as a function of Γ with fixed values of k_A and (B) as a function of k_A with fixed values of Γ. The dotted line in (A) represents a slope of 1 in logarithmic scale.

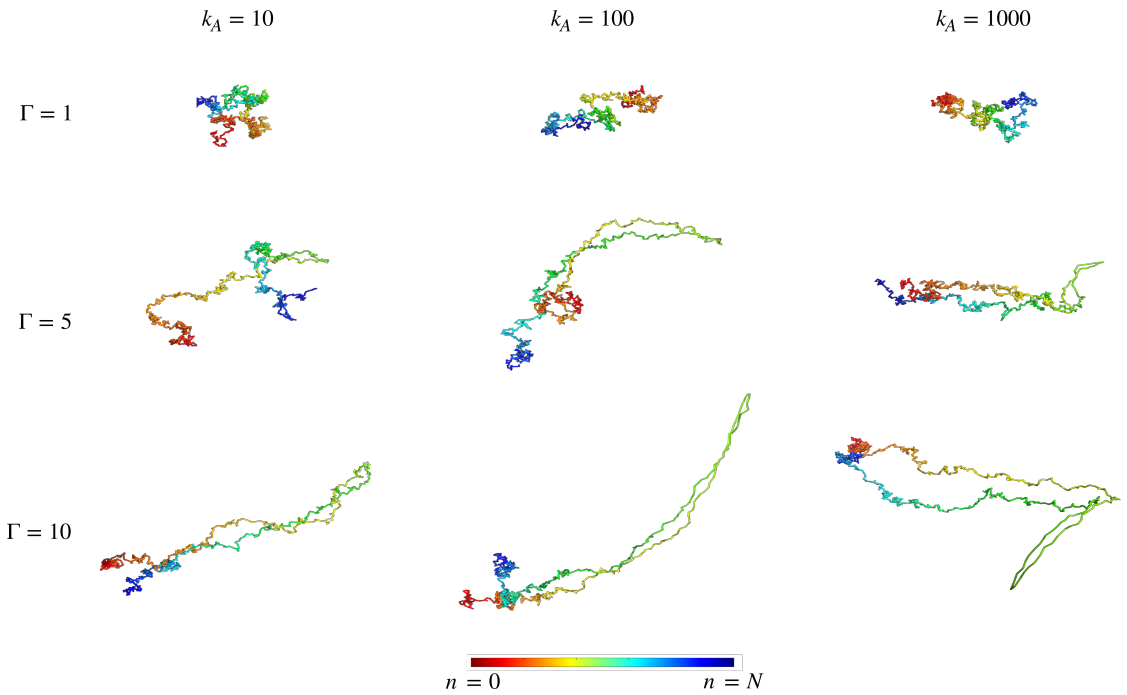

Fig. 6 Conformation of a polymer subject to local active fluctuation at the middle of the chain (i.e. $n_0 = 0.5N$) as a function of Γ and k_A. The color of the segment represents its position along the chain as shown in the colorbar .

gyration of a Rouse chain, given by

$$(R_g^2)^{\text{ex}} = \sum_{p=1}^{\infty} C_{pp}(0) - \frac{Nb^2}{6}. \tag{15}$$

We find that the excess squared radius of gyration is linearly proportional to Γ (Fig. 5A) but has a very weak dependence on k_A (Fig. 5B). Although a higher k_A elongates the polymer to a larger extent (as the force is higher), it elongates only a smaller portion of chain (Fig. 4 C), since the range of action decreases with k_A. These two factors offset each other in terms of the swelling of the entire chain.

Finally, we visualize the conformation of the polymers generated by the local active fluctuations in Fig. 6. We choose values of $\{\vec{X}_p\}$ from its steady-state distribution, which is a multivariate normal distribution characterized by mean zero (as there is no directional bias of the fluctuations) and covariance matrix with entries $\langle \vec{X}_p^{\text{ss}} \cdot \vec{X}_q^{\text{ss}} \rangle = C_{pq}(0)$ and construct the conformation $\vec{r}(n) = \sum_{p=1}^{p_{\max}} \vec{X}_p^{\text{ss}} \phi_p(n)$. We use $p_{\max} = 10000$ for this construction. As predicted in Figs. 4 and 5, we observe the structure to swell with an increase of Γ, and the elongation becomes more local to the source of active fluctuation with increase of k_A.

3.3 Correlation of conformation and active fluctuation

In the conformations generated in Fig. 6, we observed that the presence of active fluctuations swells and elongates the structure in a consistent direction. Moreover, as the active fluctuation contributes only to the even modes for this specific case (Supplementary Fig. S1), the elongation demonstrates symmetry with respect to the source of the active fluctuation, creating hairpin-like structures. We proceed to determine whether the conformation of the structure is influenced by the direction of the active fluctuation. We numerically simulate Eq. 1 (Supplementary Material note 3) and track both the polymer position as well as the direction of

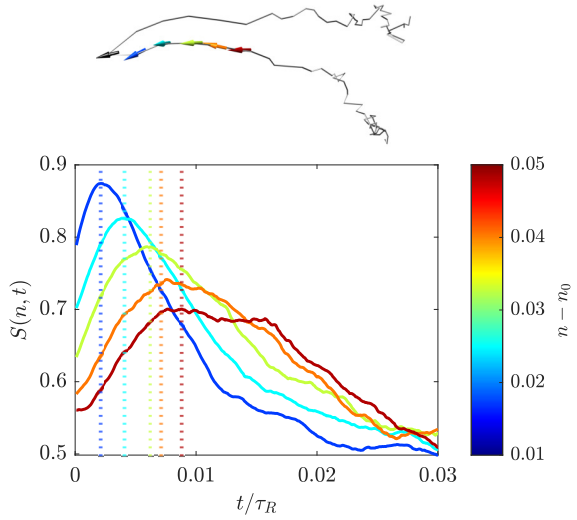

Fig. 7 Correlation of the active fluctuation and local conformation at a specific segment as a function of time delay t averaged over multiple simulations conducted with parameters $\Gamma = 10$, and $k_A = 100$. The colors correspond to segments at different distances from the source of the active fluctuations, as shown in the colorbar. Dotted lines mark the time $t_{\max}(n - n_0)$, which corresponds to the maxima of $S(n,t)$. Above the plot, we show a conformation of a polymer at time 0 in gray. The black arrow denotes the active fluctuation at n_0 at that time. The other arrows are centered at n and represent the unit vectors in the direction of active fluctuation at $-t_{\max}(n - n_0)$.

active fluctuation. Moreover, we quantify the correlation of the local tangent at segment n with direction of the active fluctuation at time t before by defining the metric

$$S(n,t) = \frac{|\vec{r}_s(n,0) \cdot \vec{f}_A(-t)|}{|\vec{r}_s(n,0)||\vec{f}_A(-t)|}, \tag{16}$$

where $\vec{r}_s(n,0) = [\vec{r}(n+\delta,0) - \vec{r}(n-\delta,0)]/2\delta$ is the local tangent at time 0, and $\vec{f}_A(-t)$ is the active fluctuation at the source n_0 at time $-t$ (i.e. before time 0).

Our calculation shows that the conformation near the source of active fluctuation is highly aligned with the direction of active fluctuation (i.e. $\lim_{n\to n_0} S(n,0) = 1$) (Fig. 7). As we move further from the source of the fluctuation, the local tangent at n becomes maximally correlated with the direction of active fluctuation at a finite time $t_{\max}(n-n_0)$ before time 0 (Fig. 7). The result shows the local tangent at the segment n at time 0 gives us an estimate of the direction of the active fluctuation at $-t_{\max}(n-n_0)$. This result suggests that the current conformation provides evidence for the past active forces, since the tangent at position n correlates to the past active force through the non-local stress propagation along the chain. We illustrate this physical effect with an example snapshot in Fig. 7. Altogether, these results highlight that the conformation at a given time contains the history of the active fluctuation.

4 Conclusions

In this article, we present an analytical theory to comprehensively examine the effects of active fluctuations with any temporal correlation and spatial correlation along the chain. We demonstrate the power of this approach by analyzing the case of active fluctuations localized at a single chain segment with exponential decay of correlation in time. We show that such active fluctuations result in a significant departure from the behavior of a Rouse chain both in terms of structure and dynamics. We quantitatively identify the length and time scale associated with such departure by comparing the effect of Brownian and active fluctuations. On the other hand, we show that the local nature of the fluctuation introduces a variation in dynamics and structure associated with the proximity to the source of the active fluctuation. Our numerical simulations have revealed that the configuration of the polymer retains a historical record of the active fluctuations.

We note that in this article, we deliberately focus on the quantities that can also be captured using contemporary experimental tools. This suggests that this framework can be utilized to infer the nature of the active fluctuation from the current experimental approaches. From the results presented in this paper, we can estimate the location and correlation time of a point active fluctuation by calculating the mean squared displacement (MSD) of tracers and the mean squared inter-spot distance (Δr^2) of multiple traces from live and fixed imaging data. Guided by this framework, we envision that inverse problems may be formulated and solved using Bayesian-inference enabled optimization techniques that will infer the spatial and temporal correlations of the active fluctuations from the trajectory of a few loci on a polymer[56,57,58]. On the other hand, within models employed to depict the overall organization of biopolymers, the active force profile, varying with monomer position, can be regarded as an input to assess its influence on the global structure.

In summation, this model empowers us to understand and interpret the spatial and temporal correlation of active fluctuations within flexible biopolymers, revealing their impact on the structure, dynamics, and eventually functionality within the living systems.

Author Contributions

A.J.S, S.D, and A.G formulated the problem and developed the theory. S.D developed the numerical simulations and analysis code. All authors contributed in writing the manuscript.

Conflicts of interest

There are no conflicts to declare.

Acknowledgements

We are grateful to Alistair Boettiger, Timothy Downing, and Elizabeth Read for valuable discussions. Funding for this work is provided by the National Science Foundation, Understanding the Rules of Life (Award Number 2022182).

Notes and references

1 A. Zidovska, *Current opinion in genetics & development*, 2020, **61**, 83–90.
2 I. Eshghi, A. Zidovska and A. Y. Grosberg, *Soft Matter*, 2022, **18**, 8134–8146.
3 S. Shin, H. W. Cho, G. Shi and D. Thirumalai, *Biophysical Journal*, 2023, **122**, 19a.
4 A. Mahajan, W. Yan, A. Zidovska, D. Saintillan and M. J. Shelley, *Phys. Rev. X*, 2022, **12**, 041033.
5 C. R. Clapier, J. Iwasa, B. R. Cairns and C. L. Peterson, *Nature reviews Molecular cell biology*, 2017, **18**, 407–422.
6 L. R. Racki and G. J. Narlikar, *Current opinion in genetics & development*, 2008, **18**, 137–144.
7 T. Nozaki, S. Shinkai, S. Ide, K. Higashi, S. Tamura, M. A. Shimazoe, M. Nakagawa, Y. Suzuki, Y. Okada, M. Sasai *et al.*, *Science Advances*, 2023, **9**, eadf1488.
8 S. E. Keenan, S. A. Blythe, R. A. Marmion, N. J.-V. Djabrayan, E. F. Wieschaus and S. Y. Shvartsman, *Developmental cell*, 2020, **52**, 794–801.
9 S. Dutta, A. L. Patel, S. E. Keenan and S. Y. Shvartsman, *Nature Computational Science*, 2021, **1**, 516–520.
10 F. Juelicher, K. Kruse, J. Prost and J.-F. Joanny, *Physics reports*, 2007, **449**, 3–28.
11 S. Banerjee, M. L. Gardel and U. S. Schwarz, *Annual review of condensed matter physics*, 2020, **11**, 421–439.
12 P. M. Bendix, G. H. Koenderink, D. Cuvelier, Z. Dogic, B. N. Koeleman, W. M. Brieher, C. M. Field, L. Mahadevan and D. A. Weitz, *Biophysical journal*, 2008, **94**, 3126–3136.
13 G. Lee, G. Leech, P. Lwin, J. Michel, C. Currie, M. J. Rust, J. L. Ross, R. J. McGorty, M. Das and R. M. Robertson-Anderson, *Soft Matter*, 2021, **17**, 10765–10776.

14 S. Wang and P. G. Wolynes, *Proceedings of the National Academy of Sciences*, 2012, **109**, 6446–6451.

15 S. Gunst and D. Tang, *European respiratory journal*, 2000, **15**, 600–616.

16 R. G. Winkler and G. Gompper, *The journal of chemical physics*, 2020, **153**,.

17 M. Abkenar, K. Marx, T. Auth and G. Gompper, *Physical Review E*, 2013, **88**, 062314.

18 H. H. Wensink, J. Dunkel, S. Heidenreich, K. Drescher, R. E. Goldstein, H. Löwen and J. M. Yeomans, *Proceedings of the national academy of sciences*, 2012, **109**, 14308–14313.

19 T. Eisenstecken, G. Gompper and R. G. Winkler, *The Journal of chemical physics*, 2017, **146**,.

20 A. Ghosh and N. Gov, *Biophysical Journal*, 2014, **107**, 1065–1073.

21 D. Saintillan, M. J. Shelley and A. Zidovska, *Proceedings of the National Academy of Sciences*, 2018, **115**, 11442–11447.

22 A.-K. Tornberg and M. J. Shelley, *Journal of Computational Physics*, 2004, **196**, 8–40.

23 S. Dutta, R. Farhadifar, W. Lu, G. Kabacaoğlu, R. Blackwell, D. B. Stein, M. Lakonishok, V. I. Gelfand, S. Y. Shvartsman and M. J. Shelley, *ArXiv*, 2023.

24 M. Di Pierro, B. Zhang, E. L. Aiden, P. G. Wolynes and J. N. Onuchic, *PNAS*, 2016, **113**, 12168–12173.

25 J. Paulsen, M. Sekelja, A. R. Oldenburg, A. Barateau, N. Briand, E. Delbarre, A. Shah, A. L. Sïrensen, C. Vigouroux, B. Buendia and P. Collas, *Genome Biology*, 2017, **18**, 1–15.

26 Q. MacPherson, B. Beltran and A. J. Spakowitz, *Proceedings of the National Academy of Sciences*, 2018, **115**, 12739–12744.

27 J. G. Wakim, S. H. Sandholtz and A. J. Spakowitz, *Biophysical Journal*, 2021, **120**, 4932–4943.

28 A. M. Chiariello, C. Annunziatella, S. Bianco, A. Esposito and M. Nicodemi, *Scientific Reports*, 2016, **6**, 1–8.

29 R. Wang, J. Mozziconacci, A. Bancaud and O. Gadal, *Current opinion in cell biology*, 2015, **34**, 54–60.

30 S. C. Weber, A. J. Spakowitz and J. A. Theriot, *Physical review letters*, 2010, **104**, 238102.

31 G. Bajpai and S. Safran, *PLOS Computational Biology*, 2023, **19**, e1011142.

32 M. Gabriele, H. B. Brandão, S. Grosse-Holz, A. Jha, G. M. Dailey, C. Cattoglio, T.-H. S. Hsieh, L. Mirny, C. Zechner and A. S. Hansen, *Science*, 2022, **376**, 496–501.

33 S. Dutta, A. Ghosh, A. N. Boettiger and A. J. Spakowitz, *Biophysical Journal*, 2023, **122**, 3532–3540.

34 S. C. Weber, J. A. Theriot and A. J. Spakowitz, *Physical Review E*, 2010, **82**, 011913.

35 S. C. Weber, A. J. Spakowitz and J. A. Theriot, *Proceedings of the National Academy of Sciences*, 2012, **109**, 7338–7343.

36 A. Goloborodko, M. V. Imakaev, J. F. Marko and L. Mirny, *eLife*, 2016, **5**, 1–16.

37 A. Martin-Gomez, T. Eisenstecken, G. Gompper and R. G. Winkler, *Physical Review E*, 2020, **101**, 052612.

38 N. Samanta and R. Chakrabarti, *Journal of Physics A: Mathematical and Theoretical*, 2016, **49**, 195601.

39 S. Brahmachari, T. Markovich, F. C. MacKintosh and J. N. Onuchic, *bioRxiv*, 2023, 2023–04.

40 K. Goswami, S. Chaki and R. Chakrabarti, *Journal of Physics A: Mathematical and Theoretical*, 2022.

41 D. Osmanović and Y. Rabin, *Soft Matter*, 2017, **13**, 963–968.

42 A. Goychuk, D. Kannan, A. K. Chakraborty and M. Kardar, *Proceedings of the National Academy of Sciences*, 2023, **120**, e2221726120.

43 D. Osmanović, *The Journal of chemical physics*, 2018, **149**,.

44 L. Natali, L. Caprini and F. Cecconi, *Soft Matter*, 2020, **16**, 2594–2604.

45 M. Doi and S. F. Edwards, *The theory of polymer dynamics*, Oxford University Press, 1988, vol. 73.

46 C. W. Gardiner *et al.*, *Handbook of stochastic methods*, springer Berlin, 1985, vol. 3.

47 G. E. Uhlenbeck and L. S. Ornstein, *Physical review*, 1930, **36**, 823.

48 A. Ghosh and A. J. Spakowitz, *Soft Matter*, 2022, **18**, 6629–6637.

49 J. M. Alexander, J. Guan, B. Li, L. Maliskova, M. Song, Y. Shen, B. Huang, S. Lomvardas and O. D. Weiner, *elife*, 2019, **8**, e41769.

50 M. B. Child, J. R. Bateman, A. Jahangiri, A. Reimer, N. C. Lammers, N. Sabouni, D. Villamarin, G. C. McKenzie-Smith, J. E. Johnson, D. Jost *et al.*, *Elife*, 2021, **10**, e64412.

51 L. J. Mateo, N. Sinnott-Armstrong and A. N. Boettiger, *Nature protocols*, 2021, **16**, 1647–1713.

52 A. Boettiger and S. Murphy, *Trends in Genetics*, 2020, **36**, 273–287.

53 F. Brochard-Wyart, H. Hervet and P. Pincus, *Europhysics letters*, 1994, **26**, 511.

54 P. Pincus, *Macromolecules*, 1976, **9**, 386–388.

55 P. Rowghanian and A. Y. Grosberg, *Physical Review E*, 2012, **86**, 011803.

56 N. Monnier, S.-M. Guo, M. Mori, J. He, P. Lénárt and M. Bathe, *Biophysical journal*, 2012, **103**, 616–626.

57 M. El Beheiry, S. Türkcan, M. U. Richly, A. Triller, A. Alexandrou, M. Dahan and J.-B. Masson, *Biophysical journal*, 2016, **110**, 1209–1215.

58 H. Weeratunge, D. Robe, A. Menzel, A. W. Phillips, M. Kirley, K. Smith-Miles and E. Hajizadeh, *Rheologica Acta*, 2023, 1–14.